Photoionization and ion cyclotron resonance studies of the reaction $C_2H_4^+ + C_2H_4 \rightarrow C_3H_5^+ + CH_3$ *

P. R. LeBreton, A. D. Williamson, and J. L. Beauchamp†

Arthur Amos Noyes Laboratory of Chemical Physics, California Institute of Technology, Pasadena, California 91125‡

W. T. Huntress

Jet Propulsion Laboratory, Pasadena, California 91103
(Received 24 June 1974)

High pressure photoionization mass spectrometry has been employed to study the ion molecule reaction $C_2H_4^+ + C_2H_4 \rightarrow C_3H_5^+ + CH_3$ at wavelengths between 700 and 1180 Å. Measurements have been made of the apparent ionization cross section of both $C_2H_4^+$ and $C_3H_5^+$ as a function of photon energy. The threshold energy for the reaction coincides with the ionization threshold of the parent ion at 10.51 eV. The reaction cross section decreases as the internal energy of the ionic reactant increases. Vibrational structure, observed in the $C_2H_4^+$ photoionization efficiency curve immediately above threshold (10.51–11.7 eV) permits a rough estimate of the change in reaction cross section with vibrational excitation. For the first three observed levels the change in cross section is $\leq$ 10%. However, for the fourth and fifth levels the cross section has dropped by approximately 25%. In the energy region between 11.7 and 12.1 eV a slight increase in the $C_2H_4^+$ photoionization efficiency curve appears which is not reflected in the $C_3H_5^+$ curve. A large increase in the photoionization efficiency curve of $C_2H_4^+$ occurs at 12.2 eV, the threshold of the $^2B_3$ first excited electronic state of the ion. A dramatic decrease is observed in the reaction probability of $C_2H_4^+$ formed at energies above 12.2 eV. The cross section for reaction in the excited $^2B_3$ state is $\leq$ 13% of the cross section for reaction in the lowest vibrational level of the ground electronic state. The observed decrease in reactivity is independent of repeller voltage at ion exit energies below 3 eV. Pressure studies reveal that after one or two collisions, the reactivity of $C_2H_4^+$ is re-established, suggesting that relaxation of internal excitation is an efficient process. The change in reactivity of $C_2H_4^+$ with internal energy is compared to the effects of translational excitation as determined using the techniques of ion cyclotron resonance spectroscopy.

I. INTRODUCTION

Ethylene ion–molecule reactions have been extensively investigated in radiolysis studies,[1,2] mass spectrometric investigations,[3–5] and in ICR[6–9] and crossed beam experiments.[10–12] The process leading to formation of $C_3H_5^+$ is exothermic by 7 kcal/mole and proceeds with a large cross section (greater than 100 Å^2) for collision energies of about 0.1 eV. Product, angle, and translational energy distributions measured in beam experiments indicate that at low collision energies ($\leq$ 4 eV relative kinetic energies) the reaction proceeds via a long-lived $(C_4H_8^+)$* intermediate.[10–12] Additional evidence for such an intermediate rests in its observation as a termolecular association product in high pressure mass spectrometric investigations[3] and its neutralization by charge scavengers to form isomeric butenes in the high pressure radiolysis of ethylene.[1,2] At higher energies the reaction undergoes a smooth transition to a direct mechanism which takes place in short collision times.[10–12]

ICR studies have been carried out to determine the dependence of the reaction rate constant upon collision energy[6,9] and upon internal energy of the $C_2H_4^+$ parent ion.[7] In the former investigation the rate constant was found to decrease by an order of magnitude when the initial translational energy was increased from thermal to 10 eV in the center of mass. In the latter set of experiments the internal energy of the $C_2H_4^+$ reactant was varied by changing the impact energy of the electron beam used for ion production. Although the limited energy resolution of the electron beam prevented a detailed investigation of the reaction probability upon the $C_2H_4^+$ internal energy, the results indicate that the rate constant (and hence the cross section) decreases with increasing electron energy.[7] This conclusion has been discussed in terms of statistical models for collision complexes which qualitatively predict the observed behavior of the reaction probability.[7,11,13,14]

In the present study, the greater energy resolution provided by photoionization techniques has been employed to obtain more detailed information about the dependence of the ethylene reaction cross section upon the parent ion internal energy. Using photoionization techniques, Warneck has studied the reaction of $C_2H_4^+$ with C_2H_4 at ionizing wavelengths of 1087 and 923 Å.[4] A reduction of the rate coefficient for $C_2H_4^+$ from 1.24×10^{-9} cm^3 molecule$^{-1}\cdot$ sec^{-1} to 0.88×10^{-9} cm^3 molecule$^{-1}\cdot$ sec^{-1} is observed at the shorter wavelength. In addition, the termolecular association product $C_4H_8^+$ is formed with lower yield.[4] Sieck and Ausloos report a decrease in the $C_2H_4^+$ rate coefficient from 0.96×10^{-9} cm^3 molecule$^{-1}\cdot$ sec^{-1} at 1165 Å to 0.85×10^{-9} cm^3 molecule$^{-1}\cdot$ sec^{-1} at 1067 and 1048 Å (argon resonance lines).[5]

Previous photoionization and photoelectron studies have elucidated several features of the molecular and electronic structure of ethylene cations.[15–18] The ground ionic state of $C_2H_4^+$ is formed by removal of a $1b_{1u}$ electron associated with C–C π bonding, and has the electronic configuration $\ldots (2a_g)^2 (2b_{3u})^2 (1b_{2u})^2 (3a_g)^2 (1b_{1g})^2 (1b_{1u})$. The photoionization cross section for the

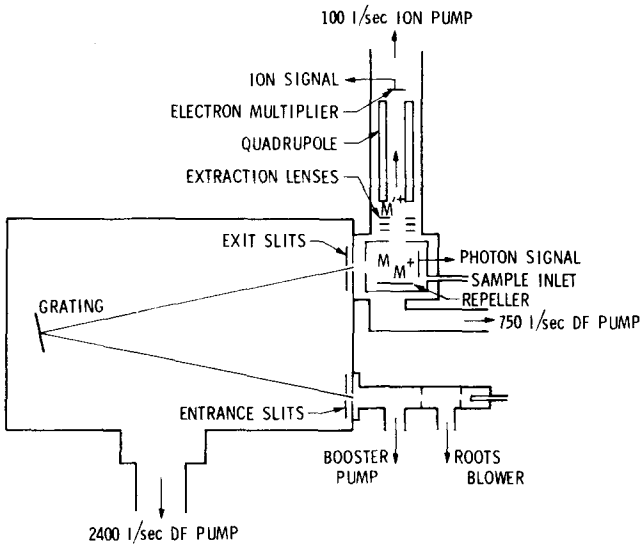

FIG. 1. Photoionization mass spectrometer. The axis of the quadrupole mass spectrometer is parallel to the exit slit of the monochromator; in the figure the mass spectrometer has been rotated 90° for purposes of illustration.

ground state exhibits vibrational structure near threshold which is associated with combinations of the C–C twisting and stretching modes.[18]

Below the threshold of the first excited state a slight increase occurs in the photoionization cross section which is possibly due to autoionization from Rydberg series leading to excited ionic states.[15,17] However, the vibrational structure associated with the ground and first excited state, which appears in the photoionization cross section between 12.2 and 13.0 eV, suggests that most $C_2H_4^+$ is formed by direct ionization.[15,17] This conclusion is supported by the results of isotopic studies in which the relative ionization efficiency curves of C_2H_4 and C_2D_4 were compared over a wide energy region (10.4–11.8 eV).[16] The identification of the first excited electronic state of $C_2H_4^+$ is uncertain but is probably formed by removal of either a $1b_{1g}$ electron, which is associated with C–H bonding, or a $3a_g$ electron, which contributes to both C–H and C–C bonding. Higher excited states whose thresholds appear at 14.4 and 15.6 eV in the ethylene photoelectron spectrum also lie in the energy region investigated in the present experiments.

II. EXPERIMENTAL

ICR experiments performed in conjunction with the present study utilized instrumentation at both Caltech and JPL. The instrumentation and experimental techniques have been previously discussed in detail.[9,19,20]

The photoionization apparatus[21] (Fig. 1) is equipped with a Hinteregger discharge lamp, a McPherson model 225 1-m normal incidence monochromator, and an Extranuclear quadrupole mass spectrometer. Dispersed light from the monochromator enters a differentially pumped reaction chamber which can be operated at pressures up to 5.0×10^{-3} torr. The sample gas flows into the chamber through a variable leak, and the chamber pressure is measured with a model 90H1 MKS Baratron capacitance monometer. Electrostatic extraction lenses outside the chamber and a repeller plate inside are used to direct ions toward the entrance aperture of the mass spectrometer. A cross section of the extraction region perpendicular to the direction of light propagation is shown in Fig. 2. The U-shaped repeller surrounds the shaded region in which ions are formed. Equipotentials are plotted for a repeller voltage of 1.0 V with respect to the source chamber. From the equipotentials it is evident that the average ion exit energy is 73% of the applied repeller voltage. The average ion exit energy is an important parameter characterizing ion–molecule reaction product distributions and apparent cross sections. Following the usual analysis for this type of source, the apparent reaction cross section, Q, is defined by Eq. (1),

$$I_p = (I_p + I_s)\ \exp(-nQl)\ , \tag{1}$$

where I_p and I_s are the ion currents associated with primary and secondary ions in the case that a single reactant leads to a single product, n is the number density of neutral reactants, and l is the mean distance (1.03 cm) from the photon beam to the ion exit aperture. The light intensity emerging from the exit slit of the monochromator and entering the chamber was measured by monitoring photoelectric emission from a platinum electrode located in the reaction chamber. The output signals of both the photon and ion detectors were measured with Cary vibrating reed electrometers. All measurements of photon intensities are corrected for the wavelength dependence of the photocathode detection efficiency.[22]

In the present experiments, the hydrogen many-line spectrum, which produces intense light in the wavelength region 900–1670 Å, and the Hopfield continuum of He, which yields continuous strong radiation between

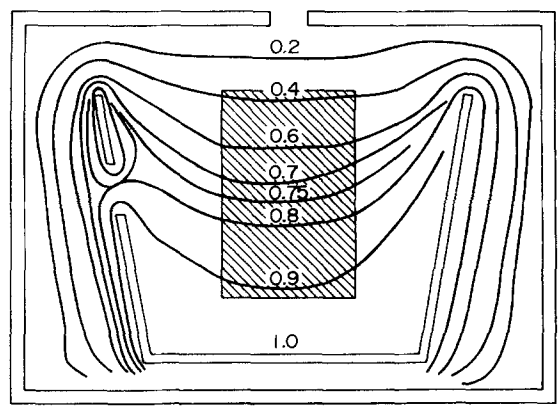

FIG. 2. Scale drawing showing cross section of source housing and repeller normal to the photon flux (shaded region). The interior dimensions of the source housing are 3.18 cm width ×2.22 cm height. Equipotentials are shown for a repeller setting of 1.0 V with respect to the source housing. The aperture in the repeller admits an electron beam from an electron gun mounted on the source housing. Extraction lenses (not shown) are mounted on the source housing and will slightly perturb the fields in the vicinity of the ion exit aperture.

1000 and 600 Å, were used to produce photons over the energy region investigated. The monochromator entrance and exit slits were set at 100 and 300 μ respectively. This resulted in a measured resolution of 3 Å or 0.02 to 0.15 eV in the wavelength region scanned. A MgF_2 coated grating blazed at 1200 Å and ruled with 1200 lines mm^{-1} was used in first order for the present experiments.

Photoelectrons produced at the photon detector gave rise to a small background ion signal at masses corresponding to both the reactant and product ions. This background signal arises from $C_2H_4^+$ formed by electron impact. It was possible to estimate the magnitude of this background by measuring the ion signals at photon energies below the $C_2H_4^+$ photoionization threshold. For photon energies greater than 10.6 eV it is estimated that the fraction of ions produced from photoelectrons is ~7% for $C_2H_4^+$ and ~3% for $C_3H_5^+$. A test was performed to determine whether the photoelectron background signal seriously affected measurements of the dependence of the reaction cross section ionizing energy. This was carried out by applying a positive voltage to the Pt photocathode, thus suppressing the background signal. For this experimental configuration it was not possible to measure the light signal. However, measurements of the ratio of product to parent ion signals over the entire energy range were consistent with measurements obtained in the normal configuration, with the photocathode unbiased.

The collision chamber of the mass spectrometer is also equipped with an electron beam at right angles to the photon beam. Electron impact ionization of the sample gas provides a simple means of tuning the mass spectrometer and determining the sensitivity of the detection system at different masses. The latter corrections are derived by comparing fragmentation patterns to those recorded without mass discrimination using the ICR apparatus.

Both the photoionization and the ICR experiments were performed at ambient temperatures (20–25 °C).

III. RESULTS

A. ICR study of C_2H_4

The thermal ion energy reactions of ethylene have not previously been characterized using trapped ion[20] ICR techniques. The variation of ion abundance with time at 11.0 eV electron energy and at 7.0×10^{-7} torr is shown in Fig. 3.[23] Reactions of the parent ion lead to the formation of $C_3H_5^+$ and $C_4H_7^+$ in the ratio 10:1 [Reactions (2) and (3)]. The product ion of Reaction (2) reacts further with C_2H_4 to form $C_5H_7^+$. The $C_5H_9^+$ intermediate in Reaction (4), which can be collisionally stabilized at 10^{-4} torr,[6] is not observed at low pressures. From the average of five determinations, the observed rate coefficient for the disappearance of $C_2H_4^+$ is $8.0\pm1.0\times10^{-10}$ cm^3 $molecule^{-1}\cdot sec^{-1}$ at 11.0 eV. At higher electron energies (13.0 eV) there is a slight upward curvature in the $C_2H_4^+$ decay curve.

$$C_2H_4^+ + C_2H_4 \longrightarrow \begin{cases} C_3H_5^+ + CH_3 & (2) \\ C_4H_7^+ + H & (3) \end{cases}$$

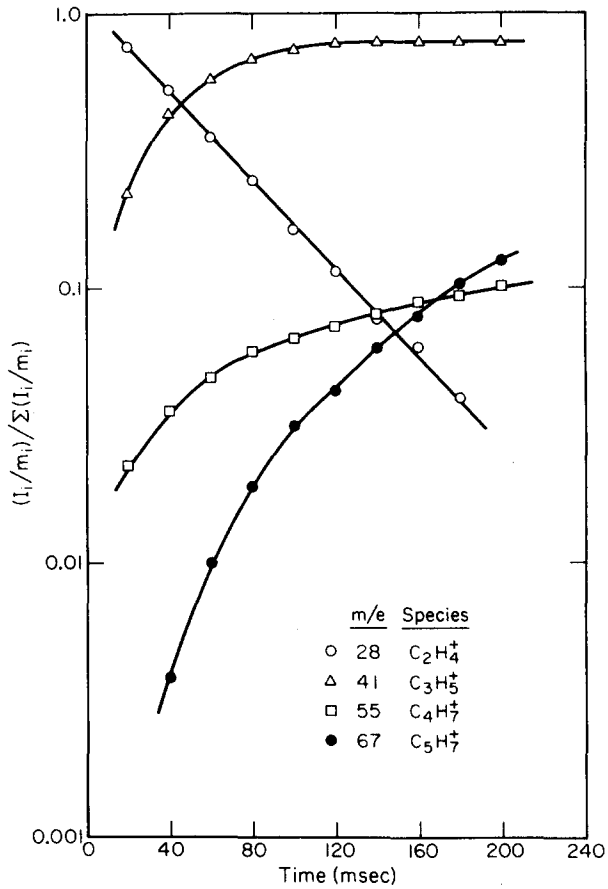

FIG. 3. Variation of ion abundance with time following ionization of ethylene at 7.0×10^{-7} torr with a 6.0 msec electron beam pulse at 11.0 eV.

$$C_3H_5^+ + C_2H_4 \longrightarrow C_5H_7^+ + H_2 \quad (4)$$

$$C_2H_2^+ + C_2H_4 \longrightarrow C_2H_4^+ + C_2H_2 \quad (5)$$

Above fragmentation thresholds for $C_2H_4^+$ formation the occurrence of Reaction (5) leads to a fairly pronounced upward curvature in the $C_2H_4^+$ decay curve, consistent with previous observations.[3,6] The upward curvature in the $C_2H_4^+$ decay curve is almost entirely removed when $C_2H_2^+$ (and $C_2H_3^+$, which also makes a small contribution) is ejected from the cell. An upward curvature in the $C_2H_4^+$ curve would be expected if a fraction of the ions formed in unreactive excited states undergo one or more collisions which relax their internal excitation and reestablish the reactivity expected for thermal ions formed near the ionization threshold. The observed effect was so small, however, that the production of excited states with modified reactivity could not be quantitatively assessed.

The effects of translational energy on the reactions of $C_2H_4^+$ with C_2H_4 and its variously deuterated analogs have previously been investigated using ICR techniques.[9] The variation of rate coefficients for individual reation channels with ion kinetic energy is indicated in Fig. 4. It has previously been suggested that twice the charge transfer rate coefficient [Reaction (6)]

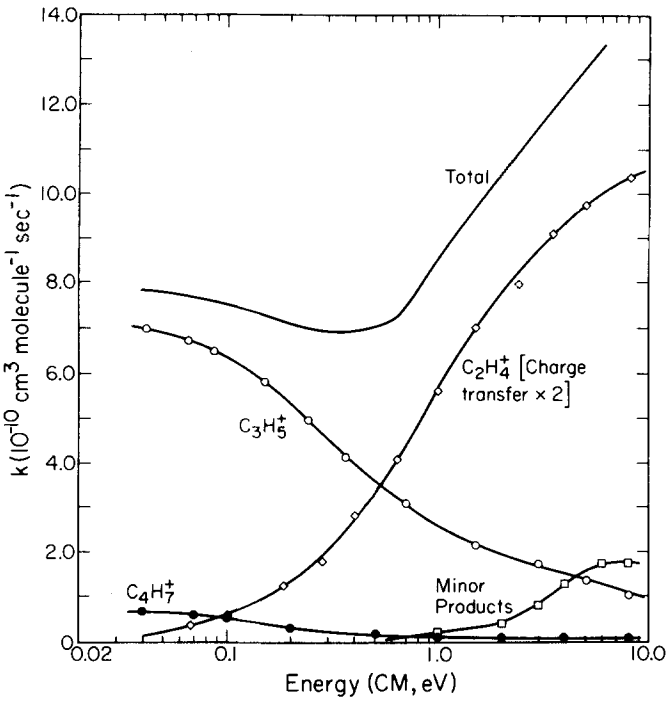

FIG. 4. Variation with relative kinetic energy of the product distribution for reactions of $C_2H_4^+$ with C_2H_4 (data from Ref. 9).

$$C_2H_4^+ + C_2D_4 \rightarrow C_2H_4 + C_2D_4^+ \quad (6)$$

can be taken as a measure of collisions in which the reactants interact strongly without leading to product formation, possibly forming an intermediate complex which dissociates to regenerate the reactant ions.[6] The product curve labelled $C_2H_4^+$ in Fig. 4 is produced in this fashion. Including this in the total leads to a rate coefficient nearly independent of ion energy up to 0.75 eV in the center of mass. At 0.75 eV in the center of mass, reaction is occurring at impact parameters less than ~3.6 Å, approaching the hard sphere collision radius of the reaction partners. Above 0.75 eV, the total rate coefficient increases with increasing ion energy, owing predominately to the increase in the charge transfer process.

B. Variation of apparent ionization and reaction cross sections with photon energy

Figure 5 shows the apparent ionization cross sections of $C_3H_5^+$ between 1179 and 800 Å. Also given are the thresholds for the fragments C_2H_2 and $C_2H_3^+$ which occur at 13.13 and 13.25 eV, respectively.[7] The data in Fig. 5 are normalized with respect to photon intensity. By frequently measuring ion and light signals at a reference wavelength, changes in the reaction chamber pressure could be detected.

For wavelengths near the ionization threshold of ethylene where prominent vibrational structure is observed, measurements were taken at 1 Å intervals. For wavelengths below 1140 Å where structure in the $C_2H_4^+$ cross section is less pronounced, measurements were taken at 5 Å intervals. The main features of the $C_2H_4^+$ curve, including the ionization threshold at 10.51 eV, the gradual rise in the photoionization efficiency in the region 11.7 to 12.1 eV, and the large increase due to the onset of the first excited electronic state at 12.2 eV, are in agreement with previously reported results.[15–17] At the thresholds for highly excited electronic states, which appear at 14.4 and 15.6 eV in the photoelectron spectrum of ethylene, a dramatic change in the curve such as that observed for the first excited state does not occur.

In Fig. 5 the apparent cross section of $C_3H_5^+$ has been normalized to the $C_2H_4^+$ cross section at 1161 Å. In the low energy region the parent and product ion curves are similar and share the same threshold. However, above 10.7 eV the $C_3H_5^+$ curve becomes gradually lower than the parent ion curve, denoting a decrease in the reaction cross section. At energies above 12.2 eV, the large increase of the $C_2H_4^+$ curve corresponding to population of the first excited electronic state,[18] is only partly reflected in the $C_3H_5^+$ curve. The presence of the fragment ions $C_2H_2^+$ and $C_2H_3^+$ is not a problem since they do not react directly with C_2H_4 to produce $C_3H_5^+$. This conclusion is supported by the fact that no prominent structure is observed in the $C_3H_5^+$ ionization curve at the thresholds for the fragments.

Figure 6 shows the $C_2H_4^+$ amd $C_3H_5^+$ ionization cross section curves expanded in the region 1179–1135 Å. The positions of the vibrational steps observed in the $C_2H_4^+$ curve at 1174, 1162, 1155, and 1144 Å are in agreement with those reported earlier.[15–17] The stepwise structure observed in the parent ion is reflected in the product $C_3H_5^+$ curve. The step heights corresponding to the first three vibrational states are approximately the same for the parent and product ions and the separation of the curves is very small. For the fourth and fifth states, however, the separation is greater.

Figure 7 shows the variation of the apparent reaction cross section with ionizing energy over the entire wavelength region studied. In constructing Fig. 7, only the product $C_3H_5^+$ was considered. In the photoionization experiments this species accounts for 92% of the total product ion signal due to $C_2H_4^+$ reactions. In addition to the photoionization results, Fig. 7 contains the ICR electron impact data obtained by Gross and Norbeck[7] in their study of the variation of reactivity with parent ion internal energy. The two sets of data show qualitative agreement, as discussed further below.

C. Variation of apparent reaction cross section with repeller voltage

The apparent change in cross section with photon energy should reflect changes in reactivity due to internal excitation of the reactant ion. The apparent effect of internal excitation on reactivity may also depend on the translational energy of the reactant ion. The design of the photoionization apparatus is such that the reactant ion will be continuously accelerated between the point of formation and the ion exit aperture. Hence the translational energy is poorly defined. The qualitative effect of translational energy can be investigated by varying the repeller voltage and observing the change in the apparent cross section. Such experiments for

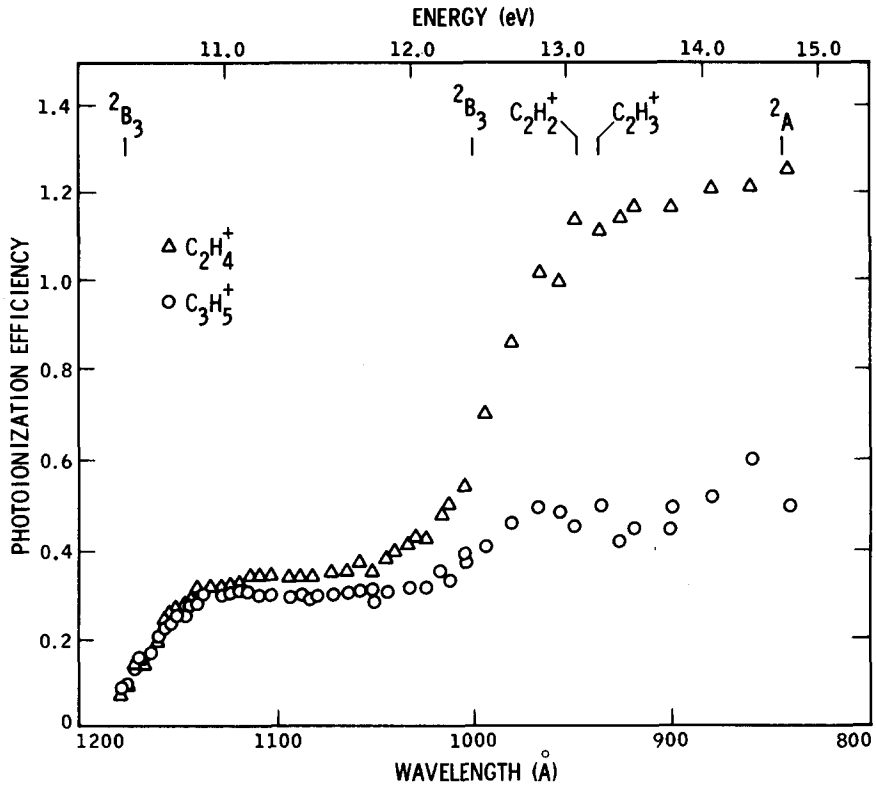

FIG. 5. Apparent photoionization cross sections for $C_2H_4^+$ and $C_3H_5^+$ normalized at 1161 Å. Data from 1180–900 Å were taken with the hydrogen many-line spectrum; data below 900 Å were taken with the Hopfield He light source. Arrows denote thresholds for the fragments $C_2H_2^+$ and $C_2H_3^+$. Repeller voltage 4.0 V.

$C_2H_4^+$ formed by electron impact have been reported by Field, Franklin, and Lampe[3] who observe that the apparent cross section decreases somewhat more rapidly than $E^{-1/2}$ where E is the ion exit energy. This is expected for a process with a rate constant which decreases with increasing ion-neutral relative kinetic energy. In the present study we have reinvestigated the effect of repeller voltage on *relative* cross section at 1161 and 969 Å. The results are shown in Fig. 8 and demonstrate that the observed decrease in reaction cross section with internal energy above the first excited state of $C_2H_4^+$ is constant for repeller voltages less than 4 V, corresponding to an ion exit energy of 3 eV. The data in Fig. 8 were recorded at low conversion (< 10%) to avoid observation of products in secondary collisions.

D. Variation of apparent reaction cross section with pressure at selected wavelengths

Although the relatively large apertures in the ion source prevented the use of higher pressures, the variation of ion abundance with pressure could be investigated up to 10^{-2} torr. Such data are shown in Fig. 9 for the two wavelengths 1161 and 969 Å. At the longer wave-

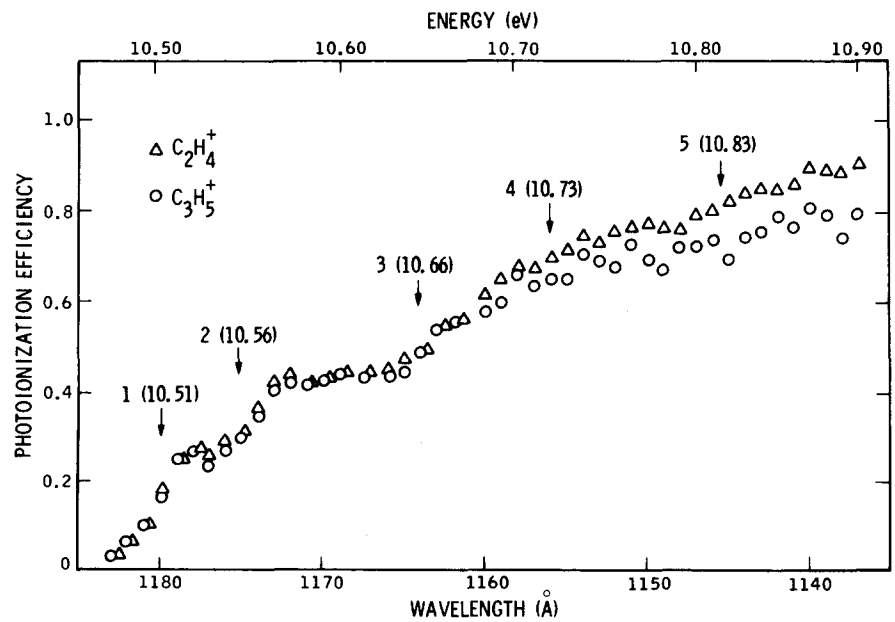

FIG. 6. Apparent photoionization cross sections for $C_2H_4^+$ and $C_3H_5^+$ in the energy region 10.5 to 10.9 eV recorded at ~10% conversion. Data for the two ions are normalized at 1161 Å. Arrows indicate thresholds of vibrational levels arising from combination modes of $C_2H_4^+$. The separation of the two sets of data above 10.7 eV denotes a decrease in reaction cross section with increasing $C_2H_4^+$ vibrational energy. Repeller voltage 4.0 V.

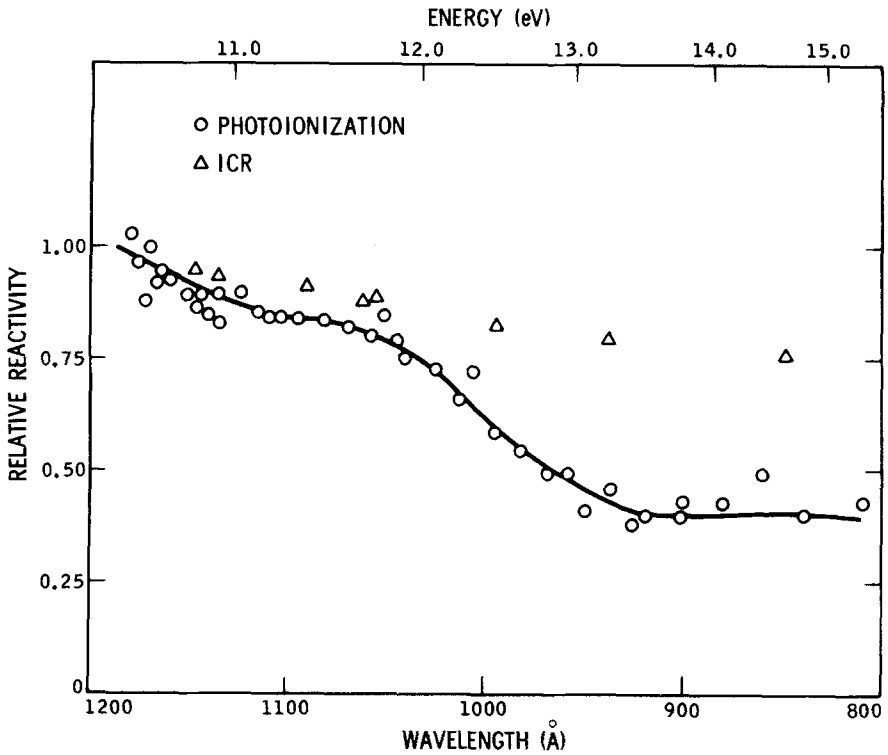

FIG. 7. Relative total reaction cross section for $C_2H_4^+ + C_2H_4 \rightarrow C_3H_5^+ + CH_3$ for photon energies between 10.5 and 15.7 eV. Triangles denote ICR data taken from Ref. 7. The two sets of data show qualitative agreement, as discussed in the text.

length a reasonably linear decay of $C_2H_4^+$ is observed, the slope being related to the apparent cross section. At the shorter wavelength, above the first threshold for formation of the first excited state of $C_2H_4^+$, the initial slope (low pressure) is considerably less than the slope observed at 1161 Å, consistent with the data shown in Figs. 5 and 7. At higher pressures, however, it is evident from the data in Fig. 9 that there is an increase in slope and hence in apparent reaction cross section. This can be attributed to an increased reactivity of initially excited $C_2H_4^+$ ions which have undergone nonreactive collisions with C_2H_4 neutrals.

A simplified reaction scheme serves to describe the initial formation of excited nonreactive [Process (7)] and reactive [Process (8)] $C_2H_4^+$ ions. The latter are assumed to be reactive, forming $C_3H_5^+$ in Reaction (9) with cross section Q_r.

$$C_2H_4 + h\nu \longrightarrow \begin{cases} (C_2H_4^+)^e + e & (7) \\ (C_2H_4^+)^r + e & (8) \end{cases}$$

Excited nonreactive ions are deactivated in nonreactive collisions [Process (10)] with cross section Q_d and react in subsequent collisions.

$$(C_2H_4^+)^r + C_2H_4 \xrightarrow{Q_r} C_3H_5^+ + CH_3 \quad (9)$$

$$(C_2H_4^+)^e + C_2H_4 \xrightarrow{Q_d} (C_2H_4^+)^r + C_2H_4 \quad (10)$$

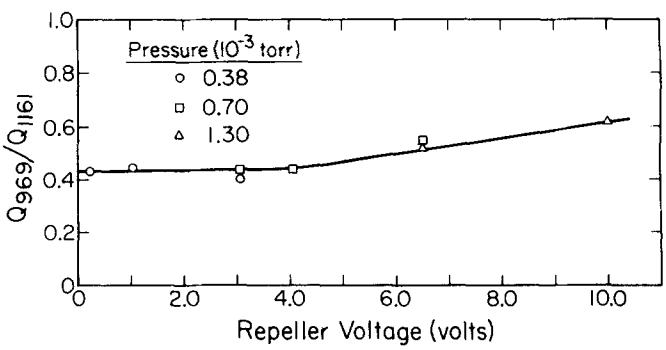

FIG. 8. Effect of repeller voltage on the ratio of apparent reaction cross sections for $C_2H_4^+ + C_2H_4 \rightarrow C_3H_5^+ + CH_3$ at 969 and 1161 Å.

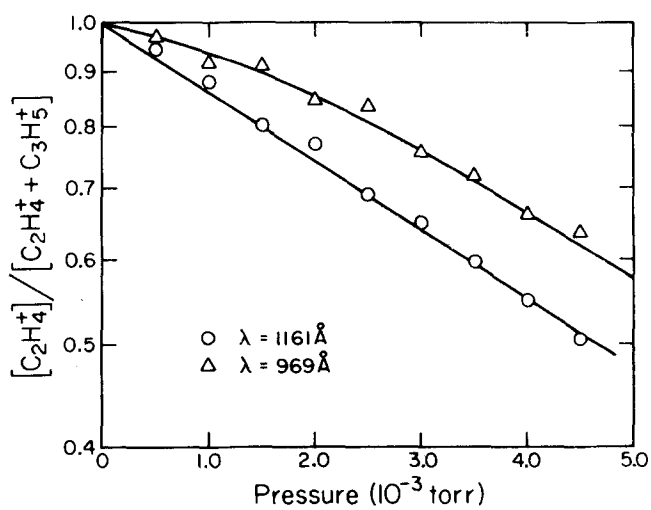

FIG. 9. Variation with pressure of the relative abundance of $C_2H_4^+$ at 969 and 1161 Å. The lines through the experimental data points represent the best fit obtained with Eq. (11) in the text.

Since $(C_2H_4^+)^e$ and $(C_2H_4^+)^r$ are not distinguished by the detection system, the fractional concentration of remaining $C_2H_4^+$ at the exit aperture will be given by the solution of the differential equations governing ion concentrations in the ion source. The result is given by Eq. (11), where $(C_2H_4^+)_0^e$ and $(C_2H_4^+)_0^r$ are the initial concentrations of ions produced in Processes (7) and (8) respectively.

$$\frac{C_2H_4^+}{C_2H_4^+ + C_3H_5^+} = \frac{[(C_2H_4^+)_0^r(Q_r - Q_d) + (C_2H_4^+)_0^e(Q_r e^{-n(Q_d - Q_r)l} - Q_d)]e^{-nQ_r l}}{(Q_r - Q_d)(C_2H_4^+ + C_3H_5^+)}. \tag{11}$$

Note that if $Q_d > Q_r$, the slope of the 969 Å ion decay curve shown in Fig. 9 will be proportional to Q_r at high pressure. Although the data are somewhat limited by inability to achieve higher pressures, the slopes of the 969 and 1161 Å curves at higher pressure appear to be approximately equal. The slope for the decay of $C_2H_4^+$ at 1161 Å gives an apparent reaction cross section of 44 Å^2, in fair agreement with the values 33 Å^2 reported by Tiernan and Futrell and 40 Å^2 reported by Wexler and Marshall.[3] Taking $Q_r = 44$ Å^2 at 969 Å, the best fit (shown in Fig. 9) is obtained with $Q_d = 4.2Q_r = 183$ Å^2 and $(C_2H_4^+)_0^r$ and $(C_2H_4^+)_0^e$ being 30% and 70% of the initially formed ions, respectively. This analysis, with its inherent approximation, indicates that relaxation of internal excitation is very efficient, the large value of Q_d suggesting that a single collision sufficies to deactivate the ions and re-establish their reactivity.

IV. DISCUSSION

As noted in the Introduction, Warneck[4] reports a decrease of 30% in the rate coefficient for $C_2H_4^+$ in comparing reactivity at 923 Å to that observed at 1087 Å. The present measurements indicate an even larger decrease in the apparent reaction cross section at the corresponding wavelengths. Because of the range of wavelengths utilized in the present experiments it is possible to discern that this change of reactivity occurs in three distinct energy regions: (1) the threshold region below 10.9 eV, (2) the intermediate energy region between 11.7 and 12.2 eV, and (3) the high energy region above 12.2 eV. Figure 6 indicates that small decreases are observed in the total reaction cross section for ionizing energies lying in the threshold region where $C_2H_4^+$ vibrational structure is observed. A rough estimate of the relative cross section of each of the levels can be carried out by assuming that the photoionization efficiency for population of a given vibrational state remains constant above its threshold. In this manner it is found that the cross section for the second and third levels are approximately the same as that for the first level, decreasing by less than 10%. However, at higher levels the change is greater; the cross section for reaction in the fourth and fifth levels decreases by ~25%.

In the intermediate energy region Fig. 5 indicates that the apparent reaction cross section decreases significantly, being ~ 25% lower than at threshold for an ionizing energy of 12.1 eV. In this region the small increase in the $C_2H_4^+$ ionization efficiency curve, coupled with the absence of a similar increase in the $C_2H_5^+$ curve and the lack of structure in the photoelectron spectrum, suggest that a small amount of $C_2H_4^+$ is being produced by autoionization. The results indicate that the additional parent ions produced in this region are in excited vibrational states which are less reactive than ground state ions.

In the high energy region above the threshold of the first excited electronic state the apparent reaction cross section decreases dramatically. The apparent decrease in reactivity is very sensitive to the extent of conversion due to the rapid deactivation of excited nonreactive ions as noted above. By comparing steps heights in photoionization efficiency curves for $C_2H_4^+$ and $C_3H_5^+$ recorded at 5% conversion it is estimated that the cross section for reaction in the excited $^2B_3$ state is $\leq 13\%$ of the cross section for reaction in the lowest vibrational level of the ground electronic state. For this measurement it is difficult to insure that no deactivating collisions take place. For example, the data shown in Fig. 5, recorded at 10% conversion, indicate that the cross section is $\leq 23\%$ of the ground state value. The nature of the internal excitation is not well characterized. The general assumption is that radiationless processes lead to vibrationally excited ground states when ions are generated initially in electronically excited states. Emission from the lowest excited electronic state, which should have been populated in a number of different experiments, has not been observed.[24] Hence the radiative lifetime is not known. For radiative lifetimes greater than 10^{-5} sec, it is estimated that the majority of collisions in the photoionization experiments would involve electronically excited $C_2H_4^+$. At photon energies above 14.4 and 15.6 eV, which are the thresholds for higher excited electronic states of $C_2H_4^+$, no structure was observed in the $C_3H_5^+$ ionization cross section. Since both of these states lie above fragmentation thresholds of the parent ion, it is likely that they are depleted by unimolecular dissociation processes which should be fast compared to the time scale for reactive collisions.

The ICR data shown in Fig. 7 shows qualitative agreement with the photoionization experiment. Quantitative comparisions are not meaningful due to the unknown distribution of states in the electron impact ionization and to the different threshold behavior and energy resolution of the two techniques. However, the ICR results are interesting due to the different time scales of the two experiments (collision times are $\sim 5 \times 10^{-6}$ and 10^{-3} sec in the photoionziation and ICR experiments, re-

spectively). The fact that Gross and Norbeck observe a decrease in reaction cross section similar to our results indicates that radiative decay of excited $C_2H_4^+$ is not complete after 10^{-3} sec.

The present results indicate that the reaction cross section for production of $C_3H_5^+$ decreases as the internal energy of the $C_2H_4^+$ parent ion increases. This is consistent with predictions of statistical models which have been used to treat reactions that proceed through formation of an intermediate complex.[10–14] A common feature of the statistical treatments is the assumption that the lifetime of the complex is sufficiently long to permit complete radomization of internal energy, consistent with conservation laws restricting the dynamical variables in a collision.[13,14] These models predict that the number of energetically accessible states associated with each reaction channel (including in particular regeneration of the reactants) determines the manner in which the intermediate decomposes. As the number of accessible reactant states increases, the probability of nonreactive collision increases while that for reactive collision decreases, thus leading to a decrease in the apparent reaction cross section and reaction rate.

Considerable speculation regarding the nature of the intermediate in reaction (2) has been offered by various investigators. Radiolysis experiments in which isomeric butenes are trapped by neutralization provided the best evidence for the nature of the intermediate.[1,2] Since the butenes are structurally distinct from the reactants one must suppose an initial intermediate which isomerizes a to the more stable butene isomers. Weiner, Lee, and Wolfgang[12] have proposed a "protonated cyclopropane" intermediate as the initial complex to explain isotopic product distrubtions which, ignoring possible isotope effects, are significantly different from statistical. Their model fails, however, to explain the distribution of isotopic products for 1,2-ethylene-d_2.[5] Our view of the reaction intermediate is a loose tetramethylene structure as indicated in Fig. 10. The tetramethylene intermediate can undergo a rearrangement to one of the isomeric butenes or fragment to regenerate the reactants. At threshold (low internal and translational excitation), the regeneration of reactants is improbable in competition with the energetically favorable rearrangement. At higher internal energies the higher frequency factor associated with the C–C bond cleavage make it the favored reaction channel. Additional support for these conjectures comes from the recent studies[25] of the decomposition of cyclobutane ions formed with known internal energy by charge transfer from selected reagents ions A^+ [Reactions (12a)–(12c)]:

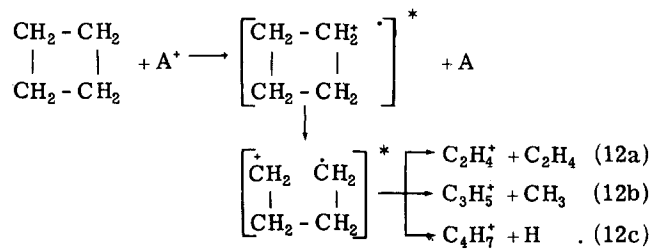

Lifshitz and Tiernan suggest that fragmentation occurs from a loose tetramethylene intermediate. With increasing internal excitation, $C_2H_4^+$ becomes the most prominent reaction product, but only from cyclobutane and not from the other C_4H_8 isomers.[25] In the first excited electronic state, $C_2H_4^+$ would form an intermediate in reaction 2 containing 2.5 eV internal excitation. With this level of excitation in the tetramethylene ion, Lifshitz and Tiernan observe the product distribution $C_2H_4^+$ (54%), $C_3H_5^+$ (36%), and C_4H_7 (10%). While our experiments suggest that $C_2H_4^+$ is more prominent, the difference may be imposed by restrictions on dynamic variables (angular momentum in particular) in forming the excited tetramethylene intermediate by reaction of C_2H_4 with excited $C_2H_4^+$. Convincing evidence for tetramethylene intermediates is presented in recently reported studies of the gas phase ion chemistry of fluoroethylenes.[26]

There are two interesting questions left unresolved by the present experiments. It is entirely possible that the charge transfer channel (involving either ground state or excited reactant ions) could occur at large impact parameters and not involve a long lived intermediate as is suggested in the present work. This could be decided in beam studies with appropriate isotopically labelled reagents. The second point concerns the nature of the internal excitation in $C_2H_4^+$ when reaction occurs. Although ionization may generate $C_2H_4^+$ in the first ex-

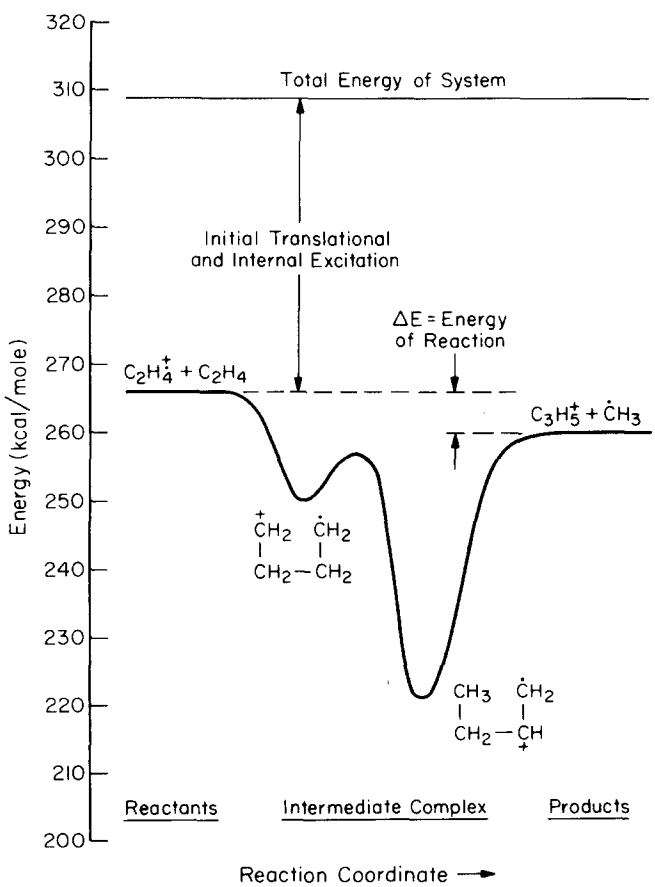

FIG. 10. Reaction coordinate diagram illustrating the energetic changes associated with the reaction $C_2H_4^+ + C_2H_4 \rightarrow C_3H_5^+ + CH_3$ involving a intermediate tetramethylene ion.

cited electronic state, the usual assumption is that initially formed excited states of polyatomic ions undergo radiationless transitions to vibrationally excited ground electronic states from which fragmentation occurs.[27] Our experiments provide no information concerning the nature of the internal excitation when reaction occurs.

*This research was supported in part by the United States Atomic Energy Commission under Grant No. AT(04-3)-767-8 awarded to J. L. Beauchamp, and presents one phase of research carried out at the Jet Propulsion Laboratory, California Institute of Technology, under Contract No. NAS7-100, sponsored by the National Aeronautics and Space Administration. The instrumentation was made possible by a grant from the President's Fund of the California Institute of Technology.

†Dreyfus Teacher–Scholar.

‡Contribution No. 4906.

[1]G. G. Meisels, J. Chem. Phys. **42**, 2328 (1965).

[2]G. G. Meisels, J. Chem. Phys. **42**, 3237 (1965).

[3]F. H. Field, J. L. Franklin, and F. W. Lampe, J. Am. Chem. Soc. **79**, 2419 (1957); F. H. Field, *ibid.* **83**, 1523 (1961); T. O. Tiernan and J. H. Futrell, J. Phys. Chem. **72**, 3080 (1968); J. J. Myher and A. G. Harrison, Can. J. Chem. **46**, 101 (1968); S. Wexler and R. Marshall, J. Am. Chem. Soc. **86**, 781 (1964).

[4]P. Warneck, Ber. Bunsen Gesellschaft **76**, 421 (1972).

[5]L. W. Sieck and P. Ausloos, J. Res. Natl. Bur. Stand. A **76**, 253 (1972).

[6]M. T. Bowers, D. D. Elleman, and J. L. Beauchamp, J. Phys. Chem. **72**, 3599 (1968).

[7]M. L. Gross and J. Norbeck, J. Chem. Phys. **54**, 3651 (1971).

[8]R. M. O'Malley and K. R. Jennings, Int. J. Mass. Spectrom. Ion Phys. **2**, 441 (1969).

[9]W. T. Huntress, J. Chem. Phys. **56**, 5111 (1972).

[10]Z. Herman, A. Lee, and R. Wolfgang, J. Chem. Phys. **51**, 452 (1969).

[11]A. Lee, R. L. Leroy, Z. Herman, and R. Wolfgang, Chem. Phys. Lett. **12**, 569 (1972).

[12]J. Weiner, A. Lee, and R. Wolfgang, Chem. Phys. Lett. **13**, 613 (1972).

[13]J. C. Light, J. Chem. Phys. **40**, 3221 (1964); J. C. Light and J. Lin, *ibid.* **43**, 3209 (1965).

[14]S. A. Safron, N. D. Weinstein, D. R. Herschbach, and J. C. Tully, Chem. Phys. Lett. **12**, 564 (1972).

[15]R. Botter, V. H. Dibeler, J. A. Walker, and H. M. Rosenstock, J. Chem. Phys. **45**, 1198 (1966).

[16]J. C. Person and P. P. Nicole, J. Chem. Phys. **49**, 5421 (1968).

[17]W. A. Chupka, J. Berkowitz, and K. M. A. Refaey, J. Chem. Phys. **50**, 1938 (1969).

[18]A. D. Baker, C. Baker, C. R. Brundle, and D. W. Turner, Int. J. Mass Spectrom. Ion Phys. **1**, 285 (1968); D. W. Turner, C. Baker, A. D. Baker, and C. R. Brundle, *Molecular Photoelectron Spectroscopy* (Wiley, New York, 1970).

[19]J. L. Beauchamp, Ann. Rev. Phys. Chem. **22**, 527 (1971).

[20]T. B. McMahon and J. L. Beauchamp, Rev. Sci. Instrum. **43**, 509 (1972).

[21]Other studies utilizing this instrumentation include J. M. Ajello, W. T. Huntress, A. L. Lane, P. R. LeBreton, and A. D. Williamson, J. Chem. Phys. **60**, 1211 (1974); S. E. Buttrill, J. Chem. Phys. **61**, 619 (1974); S. E. Buttrill, J. K. Kim, W. T. Huntress, P. LeBreton, and A. Williamson, J. Chem. Phys. **61**, 2122 (1974); and J. M. Ajello, K. D. Pang, and K. Monahan, J. Chem. Phys. **61**, 3152 (1974).

[22]J. A. R. Samson, *Techniques of Vacuum Ultraviolet Spectroscopy* (Wiley, New York, 1967).

[23]Pressures were measured as described by R. J. Blint, T. B. McMahon, and J. L. Beauchamp, J. Am. Chem. Soc. **96**, 1269 (1974).

[24]J. F. M. Aarts, C. I. M. Beenakker, and F. J. DeHeer, Physica **53**, 32 (1971).

[25]C. Lifshitz and T. O. Tiernan, J. Chem. Phys. **55**, 3555 (1971).

[26]A. J. Ferrer-Correia and K. R. Jennings, Int. J. Mass Spectrom. Ion Phys. **11**, 111 (1973).

[27]For a recent review, see M. L. Vestal in *Fundamental Processes in Radiation Chemistry*, edited by P. Ausloos (Interscience, New York, 1960), Chap. 2.